JPEDAV (2008) 29:136–140
DOI: 10.1007/s11669-007-9236-1
1547-7037 ©ASM International

Phase Diagram for the System RuO_2-TiO_2 in Air

K.T. Jacob and R. Subramanian

(Submitted October 31, 2006; in revised form July 16, 2007)

There are conflicting reports in the literature regarding solid solubility in the system RuO_2-TiO_2. To resolve this issue a few experiments were conducted in air at 1673, 1723, and 1773 K. The results show limited terminal solid solubility. There is an extended solid-state miscibility gap that intersects the decomposition curve for the RuO_2-rich solid solution generating a peritectoid reaction at 1698 K. The measured equilibrium compositions of the solid solutions are used to develop a thermodynamic description of the oxide solid solution with rutile structure. Using the subregular solution model, the enthalpy of mixing can be represented by the expression, $\Delta H^{M}/\mathrm{J \cdot mol^{-1}} = X_{TiO_2}X_{RuO_2}(34{,}100X_{TiO_2} + 30{,}750X_{RuO_2})$. The binodal and spinodal curves and *T-X* phase diagram in air are computed using this datum and Gibbs energy of formation of RuO_2 available in the literature. The computed results suggest that equilibrium was not attained during solubility measurements at lower temperatures reported in the literature.

Keywords phase diagram, thermodynamic computations, thermodynamic properties, solid solution, miscibility gap, peritectoid reaction

1. Introduction

Noble-metal-oxide-based coatings have successfully replaced many of the conventional anode materials in industrial electrochemical processes. Inclusion of non-noble-metal oxides in the coating lowers costs and imparts certain desirable characteristics such as stability and selectivity. An example is the Ti//RuO_2-TiO_2 dimensionally stable anode used in the electrolysis of brine to produce chlorine and caustic soda. The active coating consists of 30 to 40 mol% RuO_2, and the remainder is generally TiO_2, although a mixture of TiO_2 and SnO_2 is also gaining acceptance. The coating, usually a few microns, is generally applied by a sol-gel process. Approximately one-third of the world consumption of ruthenium is for electrode coating. Recently Qu et al.[1] have reported current efficiency of 60.5% at room temperature for the conversion of CO_2 to methanol (CH_3OH) using Pt electrodes coated with a composite made of RuO_2 and TiO_2/titanate nanotubes—an important result for the mitigation of the greenhouse gas in the atmosphere. The corresponding Faraday efficiencies are 40.2% using RuO_2-TiO_2 nanoparticles and 30.5% using pure RuO_2.

Based on x-ray diffraction, Comninellis and Vercesi[2] have suggested that RuO_2-TiO_2 coating forms a solid solution after annealing at 733 K. Both RuO_2 and TiO_2 have the rutile structure with similar tetragonal unit cells. The lattice parameters for RuO_2[3] are $a = 0.4491$ nm and $c = 0.3107$ nm, and for TiO_2 $a = 0.4593$ nm and $c = 0.2959$ nm. The ionic radii of Ru^{4+}(0.062 nm) and Ti^{4+}(0.0605 nm)[4] for six-fold coordination are similar. Because of the identical structures and similarity of ionic radii, significant solid solubility is expected between these oxides. Although the unit-cell volumes of RuO_2 and TiO_2 are close, the *c*/*a* ratios vary from 0.6918 for RuO_2 to 0.6442 for TiO_2. TiO_2 is a semiconductor, while RuO_2 is a metallic conductor with positive temperature coefficient of electrical resistivity.

Hrovat et al.[5] examined phase equilibria in the system RuO_2-TiO_2 in air. No ternary compound or liquid phase was identified up to 1673 K, the temperature at which RuO_2 is said to have decomposed to metallic ruthenium and oxygen gas. They found solid-state immiscibility, with terminal solid solubility limited to ~10 mol% at each end. In a follow-up study, Hrovat et al.[6] determined the extent of solid solubility in the system RuO_2-TiO_2 by firing mixtures of RuO_2 and TiO_2 at different temperatures from 1473 to 1623 K and subsequent microstructural and composition analysis using a scanning electron microscope (SEM) equipped with both energy dispersive and wavelength dispersive analyzers. For quantitative analysis of composition using wavelength dispersive spectroscopy (WDS), RuO_2 single crystals obtained by evaporation of PbO from $Pb_2Ru_2O_{6.5}$ at high temperatures were used as standards. The pressed pellets containing mixtures of RuO_2 and TiO_2 were buried in RuO_2 during firing. The particle size of the powders used and the duration of firing at different temperatures were not mentioned by Hrovat et al.[6] Attainment of equilibrium was not demonstrated by these researchers. They reported terminal solid solubility at four temperatures. The solid solubility of TiO_2 in RuO_2 was higher than that of RuO_2 in TiO_2 at all temperatures. The solid solubility was found to decrease rapidly with temperature. This variation is too steep to fit any thermodynamic model. The aim of this work was to study phase relations in the system RuO_2-TiO_2 and revise the current phase diagram. If only limited solid solubility was detected, the strategy was

K.T. Jacob and **R. Subramanian,** Department of Materials Engineering, Indian Institute of Science, Bangalore 560012, India. Contact e-mail: katob@materials.iisc.ernet.in.

to measure the solid solubility at higher temperatures, where equilibrium can be established more easily, and extrapolate the results to lower temperatures using a suitable thermodynamic model. This approach was expected to give the equilibrium solvus at lower temperatures with greater reliability than direct experiment.

2. Experimental Aspects

Starting materials used in this study were powders of TiO_2 (rutile) and RuO_2 of 99.9% purity. The oxides were heated in dry air before use: TiO_2 at 1473 K and RuO_2 at 1223 K. The starting powders were characterized by x-ray diffraction.

Phase equilibrium studies were conducted at three temperatures (1673, 1723, and 1773 K) by intimately mixing powders of RuO_2 and TiO_2 in 1:1 molar ratio in ethyl alcohol, pressing the mixture into pellets at a pressure of ~100 MPa using a steel die, and heating at the required temperature for periods in excess of 5 days. During this period, the pellets were quenched, reground, and repelletized for further heat treatment four times. The pellets were contained in a platinum crucible and buried in an oxide powder mixture of the same composition. Volatile oxides of ruthenium, RuO_3, and RuO_4 began to form when RuO_2 was heated in air at high temperatures. The composition change of the pellet was minimized by surrounding it with loose powder of the same composition. Most of the volatilization occurred from the surrounding powder. When buried in loose powder, there was no significant mass loss of the pellet during high-temperature equilibration. Preliminary experiments at 1673 K indicated that 3 days were sufficient to attain equilibrium; there was no microstructural change after this period.

Attainment of equilibrium was verified by approaching the equilibrium value from both lower and higher concentrations of TiO_2 in solid solutions. After analysis of the quenched samples equilibrated at 1673 K, they were reequilibrated at 1723 and 1773 K for 5 days in separate experiments. Similarly, pellets initially heat treated at 1773 K were subsequently held at 1723 and 1673 K for the same period. The equilibrated samples were found to be well sintered and dense. The average grain size varied from 18 to 27 μm in different samples. The compositions of the heat treated pellets were determined by electron probe microanalysis (EPMA). Pure RuO_2 and TiO_2 were used as standards. A single-crystal RuO_2 standard was prepared by the thermal decomposition of $Pb_2Ru_2O_{6.5}$ compound in flowing air at 1623 K as described in Ref. 6 because RuO_2 does not sinter well in air. A polycrystalline TiO_2 standard was prepared by sintering at 1823 K; its density was 0.98 of the theoretical value. There was no variation in composition across the grains in the equilibrated samples. In each sample, compositions of about 12 large grains were determined and the average value was taken. The compositions of samples were independent of the direction of approach or the past thermal history within experimental error of ~1 mol% of TiO_2.

3. Results

Phase analysis of the sample of average composition $X^{av}_{TiO_2} = 0.5$ equilibrated in dry air at 1673 K indicated the presence of two oxide phases, one rich in TiO_2 and the other rich in RuO_2. The XRD pattern of the sample is shown in Fig. 1(a). Two peaks are seen for each reflecting plane. The direction of the peak shift with composition depends on the (*hkl*) value. Analysis of the pattern indicates that the lattice parameter *a* increases and parameter *c* decreases with X_{TiO_2}. The compositions of these phases determined by EPMA were $X_{TiO_2} = 0.21$ (±0.008) and $X_{TiO_2} = 0.83$ (±0.012). These compositions represent the limits of terminal solid solutions for the system. The results suggest that the miscibility gap is asymmetric. Since solid solubility generally increases with temperature, the miscibility gap is expected to close at higher temperatures.

Equilibration of samples with average composition $X^{av}_{TiO_2} = 0.5$ in dry air at 1723 and 1773 K resulted in a mixture of Ru metal and an oxide phase rich in TiO_2 as shown in Fig. 1(b) and 1(c). The composition of the oxide solid solutions were $X_{TiO_2} = 0.906$ (±0.013) at 1723 K and $X_{TiO_2} = 0.955$(±0.015) at 1773 K. Most of the RuO_2 present in the original sample had decomposed, and the remainder was present in the TiO_2-rich solid solution. Clearly decomposition of one component of the oxide solid solution occurred before the closure of the miscibility gap. Intersection of the decomposition curve with the miscibility gap should result in a peritectoid reaction at a temperature between 1673 and 1723 K. The exact temperature was established by thermodynamic calculations. The equilibrium compositions determined at three temperatures in air were used to define the parameters of the solution model.

4. Phase Diagram Computation

Since the miscibility gap in the RuO_2-TiO_2 system is asymmetric, the simplest solution model that can be used is Hardy's[7] subregular model. For a strictly subregular solution, the Gibbs energy of mixing is given by:[7]

$$\Delta G^M = X_{TiO_2}X_{RuO_2}(A_1X_{TiO_2} + A_2X_{RuO_2}) + RT(X_{TiO_2}\ln X_{TiO_2} + X_{RuO_2}\ln X_{RuO_2}) \quad \text{(Eq 1)}$$

where X_{RuO_2} and X_{TiO_2} are the mole fractions of RuO_2 and TiO_2, respectively, and A_1 and A_2 are model constants, sometimes designated as interaction energies, to be determined from experimental data. The first term on the right-hand side of the equation gives the enthalpy of mixing and the second term the entropy of mixing. The entropy of mixing is assumed to be ideal. The values of A_1 and A_2 are calculated from the solubility data obtained in this study at three temperatures by an iterative procedure: A_1 = 34,100 J/mol and A_2 = 30,750 J/mol. In view of the similar ionic radius of Ru^{4+}(0.062 nm) and Ti^{4+}(0.0605 nm), the relatively large value of the enthalpy of mixing is surprising. For solid solutions with rutile structure, the enthalpy of mixing may be dependent not only on the difference in unit-cell volumes on

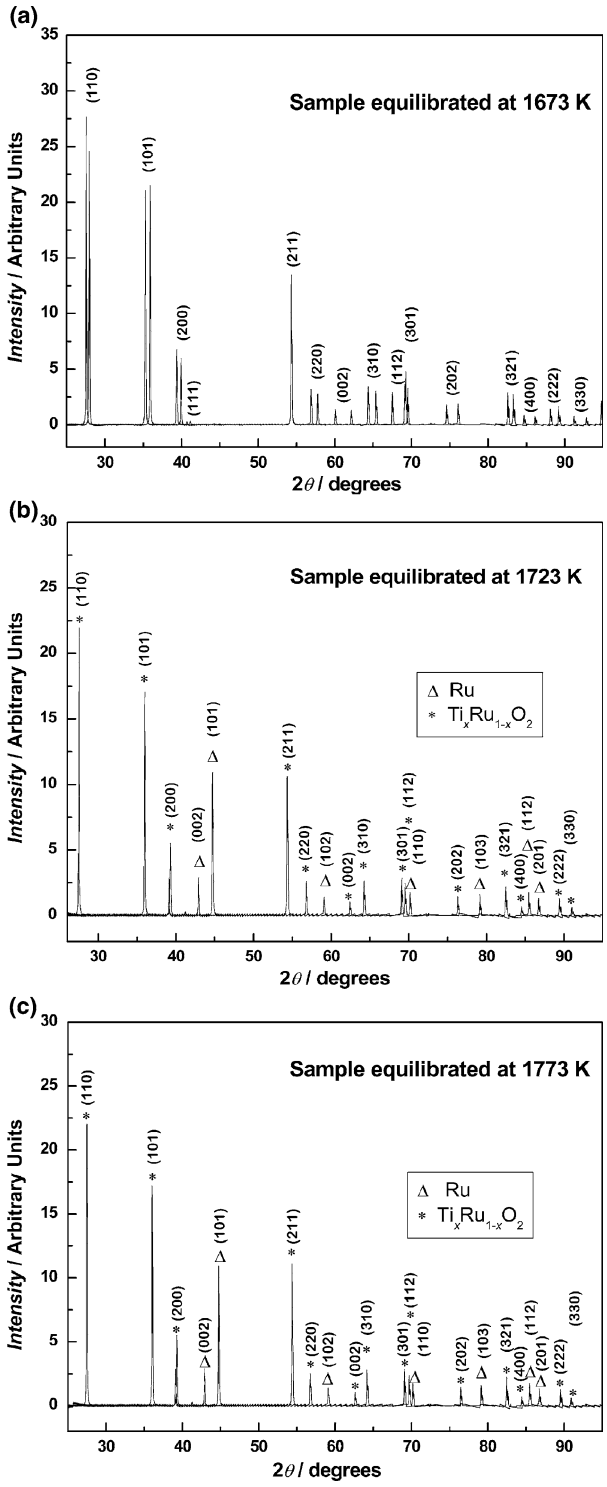

Fig. 1 XRD patterns of samples equilibrated at different temperatures: (a) at 1673 K, (b) at 1723 K, and (c) at 1773 K. The peaks are identified and indexed

the end members, but also on the difference in the *c/a* ratio. For the RuO_2-TiO_2 solid solution, the difference in *c/a* ratio is probably more significant than the difference in unit-cell volume in determining the magnitude of the enthalpy of mixing. The change in *c/a* ratio reflects the difference in the metal-oxygen (M-O) bonding. Both TiO_2 and RuO_2 crystallize in the rutile structure ($P4_2/mnm$). In the rutile structure, metal atoms are in octahedral coordination and oxygen in planar three coordination. The ideal MO_6 octahedron with six equal M-O distances is not required by symmetry in the space group $P4_2/mnm$. The local geometry is one where the M-O distances fall into two sets; four equal distances (r_4) involved in edge sharing in the chain and two (r_2) perpendicular to them. There are two types of tetragonal structure. In TiO_2 (Ti^{4+}; $3d^0$), $r_2/r_4 > 1$, and there are two long and four short M-O distances. In RuO_2 (Ru^{4+}; $4d^4$), $r_2/r_4 < 1$, with two short and four long M-O bonds. It is this difference in M-O bonding in the octahedra that is responsible for the difference in *c/a* ratio and the large enthalpy of mixing.

The relative partial Gibbs energies of RuO_2 and TiO_2 according to the subregular solution model are:[7]

$$\begin{aligned}\Delta G_{RuO_2} &= RT\ln a_{RuO_2} = RT\ln X_{RuO_2} + X_{TiO_2}^2(2A_2 - A_1) \\ &\quad + X_{TiO_2}^3(2A_1 - 2A_2) \\ &= RT\ln X_{RuO_2} + 27,400X_{TiO_2}^2 + 6700X_{TiO_2}^3\end{aligned} \quad \text{(Eq 2)}$$

$$\begin{aligned}\Delta G_{TiO_2} &= RT\ln a_{TiO_2} = RT\ln X_{TiO_2} \\ &\quad + X_{RuO_2}^2(2A_1 - A_2) + X_{RuO_2}^3(2A_2 - 2A_1) \\ &= RT\ln X_{TiO_2} + 37,450\,X_{RuO_2}^2 - 6700X_{RuO_2}^3\end{aligned} \quad \text{(Eq 3)}$$

where a_i represents the activity of component *i*. For finding the miscibility gap boundary (binodal points), the Gibbs energy of mixing ΔG^M is plotted as a function of composition X_{TiO_2} at various temperatures below the critical temperature. The composition of coexisting phases at each temperature is determined by the common tangent technique. The compositions are plotted as a function of temperature to generate the miscibility gap. The computed solvus is shown in Fig. 2 along with the experimental values obtained in this study at 1673 K and those reported by Hrovat et al.[6] at different temperatures. Although the results obtained in this study at 1673 K appear to lie on the extrapolation of the values obtained by Hrovat et al.,[6] there is sharp contrast between the solid solubilities reported by Hrovat et al. and the computed values. The temperature dependence of the solvus determined by Hrovat et al. appears to be incorrect, since extrapolation to lower temperatures would suggest negligible solid solubility at temperature near 1400 K. Probably equilibrium was not attained at the lower experimental temperatures. This suggestion is supported by the increasing difference with decreasing temperature between the experimental data of Hrovat et al. and the calculated solvus.

According to the subregular solution model,[7] the critical (consolute) temperature T_c and composition $X_{c_{TiO_2}}$ are given by:

$$A_1 = \frac{RT_c}{6X_{c_{TiO_2}}^2 X_{c_{RuO_2}}^2}\left(-9X_{c_{TiO_2}}^2 + 10X_{c_{TiO_2}} - 2\right) \quad \text{(Eq 4)}$$

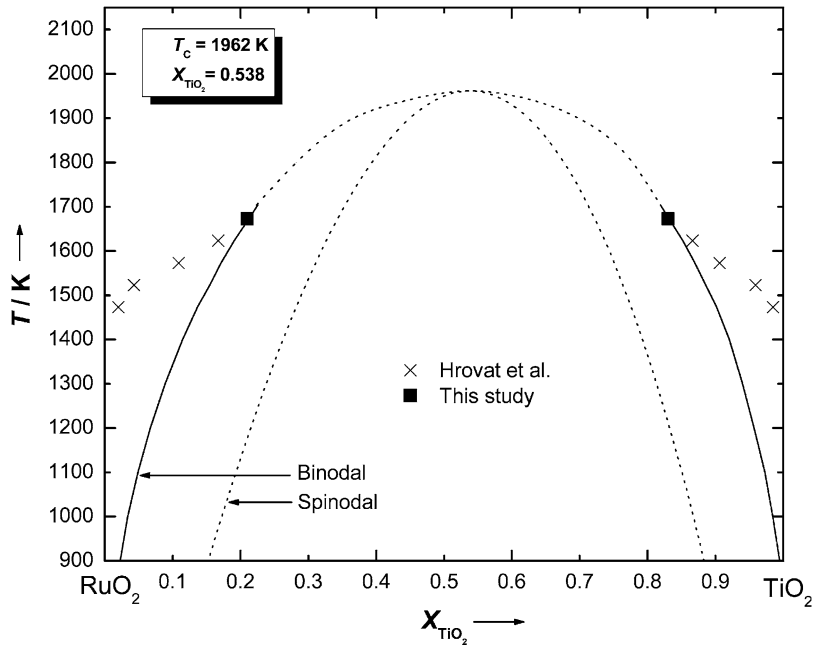

Fig. 2 Comparison of the computed miscibility gap for the system RuO_2-TiO_2 with experimental data obtained in this study and those reported by Hrovat et al.[6] The computed chemical (incoherent) spinodal curve is also displayed

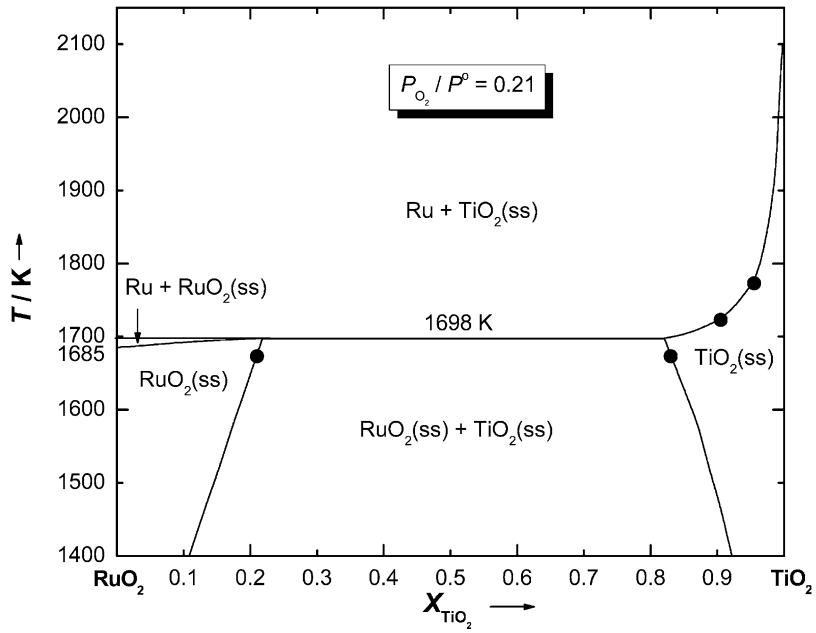

Fig. 3 Phase diagram for the system RuO_2-TiO_2 in air. RuO_2 dissociates at high temperatures to metallic Ru. Experimental data at three temperatures obtained in this study are compared with the computed phase diagram. P^o is standard atmospheric pressure (1.013×10^5 Pa)

$$A_2 = \frac{RT_c}{6X^2_{c_{TiO_2}}X^2_{c_{RuO_2}}}\left(-9X^2_{c_{RuO_2}} + 10X_{c_{RuO_2}} - 2\right) \qquad \text{(Eq 5)}$$

Noting that $X_{c_{TiO_2}} = 1 - X_{c_{RuO_2}}$ and solving the two equations above simultaneously, the critical composition and temperature are obtained: $X_{c_{TiO_2}} = 0.538$ and $T_c =$ 1962 K. Since the critical temperature is well above the decomposition temperature of RuO_2, the solid solutions will decompose and the upper part of the miscibility gap and critical temperature are not experimentally verifiable in air. However, at high pressures of oxygen the miscibility gap has physical meaning.

The chemical spinodal points are obtained by equating the second derivative of the Gibbs energy of mixing with respect to either mole fraction to zero at constant temperature. The spinodal curve satisfies the equation:

$$RT = 2X_{TiO_2}^2 X_{RuO_2}(2A_1 - A_2) + 2\,X_{TiO_2}X_{RuO_2}^2(2A_2 - A_1)$$
$$= X_{TiO_2}X_{RuO_2}(74,900\,X_{TiO_2} + 54,800X_{RuO_2}) \quad \text{(Eq 6)}$$

The computed spinodal curve is also shown in Fig. 2.

According to Jacob et al.,[3] the Gibbs energy of formation of RuO_2 from elements according to the reaction,

$$Ru + O_2 \rightarrow RuO_2$$

is given by,

$$\Delta G^o/J \cdot mol^{-1}\ (\pm 160) = RT \ln \frac{a_{RuO_2}}{p_{O_2} \cdot a_{Ru}}$$
$$= -324,720 + 354.21T - 23.49T \ln T \quad \text{(Eq 7)}$$

The decomposition temperature of pure RuO_2 ($a_{RuO_2} = a_{Ru} = 1$) in air [$(P_{O_2}/P^o) = 0.21$] calculated from the thermodynamic data is 1685 K. At higher temperatures, the decomposition product in air will be metallic Ru and an oxide solid solution in which the activity of RuO_2 has a value less than unity. The activity of Ti in equilibrium with pure TiO_2 in air at different temperatures can be computed from thermodynamic data.[8] At 1723 K, $a_{Ti} = 2.8\times10^{-19}$. The corresponding concentration of Ti in metallic Ru is expected to be negligible. Although the activity of Ti will vary with the activity of TiO_2, it is clear that the metal phase formed by the decomposition of the oxide solid solution in air is essentially pure Ru. The activity of RuO_2 in equilibrium with metallic Ru in air can be computed from Eq 7 as a function of temperature. The corresponding equilibrium composition of the oxide solid solution can be obtained from Eq 2. The computed phase diagram in air is shown in Fig. 3 along with the experimental data obtained in this study. At lower temperatures and low concentration of TiO_2, RuO_2(ss) is the stable phase. The solubility of TiO_2 in RuO_2 increases with temperature. At temperatures below 1698 K, as the fraction of TiO_2 increases a two-phase field RuO_2(ss) + TiO_2(ss) is encountered. This miscibility gap reduces with increasing temperature. At higher concentrations of TiO_2, TiO_2(ss) is the stable phase. Pure RuO_2 decomposes at a temperature of 1685 K to give metallic Ru. This decomposition temperature increases with increasing TiO_2 content of the RuO_2 solid solution. The rising decomposition temperature curve intersects the miscibility gap at 1698 K, generating an invariant peritectoid reaction. At temperatures above 1698 K, Ru + TiO_2(ss) is stable. A two-phase region of Ru + RuO_2(ss) exists between 1685 and 1698 K. The peritectoid reaction does not appear in the phase diagram for the system RuO_2-TiO_2 in air proposed by Hrovat et al.[6]

Phase diagrams at other oxygen partial pressures and oxygen potential diagrams at constant temperature can be readily computed from the thermodynamic data for the RuO_2-TiO_2 solid solution deduced in this study. It would be interesting to explore the change in phase relations when particle or grain size is reduced to the nanometer range. Further, the effect of shape of nanoparticles (e.g., nanotubes) on phase relations is an interesting area for future investigation.

5. Conclusions

An improved *T-X* phase diagram for the system RuO_2-TiO_2 in air is presented in this article. The system is characterized by a miscibility gap at lower temperatures and coexistence of metallic Ru with TiO_2-rich solid solution at higher temperatures. The two regions are linked through a peritectoid reaction at 1698 K. The solvus curves are generated by a thermodynamic model. The model parameters were obtained by fitting phase equilibrium data at three elevated temperatures generated in this study. Attainment of equilibrium was demonstrated experimentally by approaching the solid solubility limits from lower and higher compositions and temperatures. The enthalpy of mixing of the solid solution with the rutile structure is given by: $\Delta H^M/J \cdot mol^{-1} = X_{TiO_2}X_{RuO_2}(34,100X_{TiO_2} + 30,750X_{RuO_2})$. Using this information and standard Gibbs energy of formation of RuO_2 available in the literature, phase diagrams at other oxygen pressures can be computed.

Acknowledgment

One of the authors, R. Subramanian, is grateful to the Indian Institute of Science, Bangalore, for the award of Young Engineering Fellowship, which facilitated this research.

References

1. J. Qu, X. Zhang, Y. Wang, and C. Xie, Electrochemical Reduction of CO_2 on RuO_2-TiO_2 Nanotube Composite Modified Pt Electrode, *Electrochim. Acta*, 2005, **50**(16-17), p 3576-3580
2. C. Comninellis and G.P. Vercesi, Characterization of DSA-Type Oxygen Evolving Electrodes: Choice of a Coating, *J. Appl. Electrochem.*, 1991, **21**, p 335-345
3. K.T. Jacob, S. Mishra, and Y. Waseda, Refinement of Thermodynamic Properties of Ruthenium Dioxide and Osmium Dioxide, *J. Am. Ceram. Soc.*, 2000, **83**(7), p 1745-1752
4. R.D. Shannon, Revised Effective Ionic Radii and Systematic Studies of Inter-atomic Distances in Halides and Chalcogenides, *Acta Crystallogr.*, 1976, **A32**, p 751
5. M. Hrovat, J. Holc, and D. Kolar, Phase Equilibria in the RuO_2-TiO_2-Al_2O_3 and RuO_2-TiO_2-Bi_2O_3 Systems, *J. Mater. Sci. Lett.*, 1993, **12**, p 1858-1860
6. M. Hrovat, J. Holc, Z. Samardzija, and G. Drazic, The Extent of Solid Solubility in the RuO_2-TiO_2 System, *J. Mater. Res.*, 1996, **11**(3), p 727-732
7. H.K. Hardy, A Sub-Regular Solution Model and Its Application to Some Binary Alloy Systems, *Acta Metall.*, 1953, **1**, p 202-209
8. M.W. Chase, Jr., C.A. Davies, J.R. Downey, Jr., D.J. Frurip, R.A. McDonald, and A.N. Syverud, JANAF Thermochemical Tables, 3rd ed, *J. Phys. Chem. Ref. Data*, 1985, **14**(suppl. 1), p 1681